Discover Applied Sciences

RESEARCH Open Access

Metabolite profile, antioxidant, and acetylcholinesterase inhibitory evaluation of *E. crista-galli* flowers through in vitro and in silico studies

Abd. Wahid Rizaldi Akili[1], Gian Primahana[2], Sofa Fajriah[2], Ari Hardianto[1], Jalifah Latip[3] and Tati Herlina[1*]

*Correspondence:
Tati Herlina
tati.herlina@unpad.ac.id
[1]Department of Chemistry, Faculty of Mathematics and Natural Science, Universitas Padjadjaran, Jatinangor, Sumedang45363, West Java, Indonesia
[2]Research Centre for Pharmaceutical Ingredients and Traditional Medicine, National Research and Innovation Agency (BRIN), Jl. Raya Jakarta Bogor Km 46, Cibinong, West Java 16911, Indonesia
[3]Department of Chemical Sciences, Faculty of Science and Technology, Universiti Kebangsaan Malaysia (UKM), 46300 Bangi, Selangor, Malaysia

Abstract

Erythrina crista-galli is a plant species among the genus Erythrina known for their wide range if phytochemicals, particularly alkaloids and flavonoids. These phytochemicals may play potential role as antioxidant and anti-cholinesterase agents for Alzheimer's Disease (AD) treatments. This study aimed to study the metabolite profile, antioxidant and anticholinesterase activity of *E. crista-galli* flower through in vitro and in silico studies. Metabolite profiling was conducted using UPLC-MS/MS analysis, the antioxidant activity was evaluated using DPPH, ABTS, and FRAP assay, while anticholinesterase activity was evaluated using acetylcholinesterase (AChE) activity colorimetric assay, and in silico studies were conducted using both molecular docking and molecular dynamics simulation. The methanol extract from *E. crista-galli* flowers was evaluated for antioxidant activity using the DPPH, ABTS and FRAP assay, showing moderate free radical scavenging activity with IC_{50} of 153.6 ± 2.4 µg/ml in DPPH and 255.7 ± 14.9 µg/ml in ABTS assay, while 25.4 ± 1.8 mgQE/g extract in FRAP assay. The methanol extract inhibited 17.65 ± 1.28% of the AChE activity in the concentration of 50 µg/ml. Metabolite profiling via LC-MS/MS analysis revealed the presence of 16 erythrina alkaloids and 5 flavonoids in the methanol extract of *E. crista-galli* flower. Molecular docking and molecular dynamics simulations demonstrated the potency of these secondary metabolites, particularly vicenin-2 and vitexin as AChE inhibitors. This study highlights the role of *E. crista-galli* flowers as natural source of phytochemicals particularly alkaloids and flavonoids with potential antioxidant and anti-cholinesterase activity.

Article highlights

- LC-MS/MS analysis revealed the presence of flavonoids and erythrina alkaloids in methanol extract of *E. crista-galli* flower.
- The methanol extract of *E. crista-galli* flower exhibited moderate free radical scavenging activity
- A multi-faceted computational approach was conducted, combining molecular docking and molecular dynamics simulations to investigate the potency of secondary metabolites identified in *E. crista-galli flower* as AChE inhibitor.

© The Author(s) 2025. **Open Access** This article is licensed under a Creative Commons Attribution 4.0 International License, which permits use, sharing, adaptation, distribution and reproduction in any medium or format, as long as you give appropriate credit to the original author(s) and the source, provide a link to the Creative Commons licence, and indicate if changes were made. The images or other third party material in this article are included in the article's Creative Commons licence, unless indicated otherwise in a credit line to the material. If material is not included in the article's Creative Commons licence and your intended use is not permitted by statutory regulation or exceeds the permitted use, you will need to obtain permission directly from the copyright holder. To view a copy of this licence, visit http://creativecommons.org/licenses/by/4.0/.

Keywords *Erythrina crista-galli*, Metabolite profiling, Antioxidant, Alzheimer's disease, In silico

1 Introduction

Alzheimer's disease (AD) is a form of neurodegenerative disease that progressively impairs memory, thinking, and behavior. It's the leading cause of dementia, affecting millions of people globally [44]. Oxidative stress plays a pivotal role in the pathogenesis of AD, contributing to the formation of amyloid-beta plaques and neurofibrillary tangles, which are hallmark features of the disease [14]. Reactive oxygen species (ROS) generated during oxidative stress can cause significant neuronal damage, leading to cell death and cognitive impairment [48]. The excessive free radicals can interact with methionine-35 (M-35) residue of Aβ peptide. The oxidation of M-35 residue causes modification of the Aβ peptide, which leads to the formation of Aβ dimers and higher order oligomeric Aβ structures. The accumulation of oligomeric Aβ on neurons leads neuron death and neurodegeneration [46]. Antioxidants, which neutralize ROS, have been extensively studied for their potential to mitigate oxidative damage in AD [38].

In addition to oxidative stress, cholinergic dysfunction is another key factor in AD pathophysiology. The enzyme acetylcholinesterase (AChE) breaks down acetylcholine, a neurotransmitter essential for learning and memory [6]. Inhibition of AChE has been a primary therapeutic strategy for improving cognitive function in AD patients [10]. According to world health organization (WHO), there are 57 million people had dementia worldwide in 2021. This number is increasing with nearly 10 million new cases every year [57]. Currently, approximately 6.9 million Americans at the age of 65 and older live with AD. By 2060, this figure could double to 13.8 million unless significant medical advancements prevent or cure the disease [2]. With the increasing prevalence of AD, there is an urgent need for novel therapeutic approaches to halt or slow the progression of the disease. One promising avenue of research involves the exploration of natural products, particularly those with potent antioxidant and anti-cholinesterase properties. Despite extensive research efforts to discover and develop drugs for AD treatment, currently only a few that could be used for the treatment of AD, including donepezil, rivastigmine, galantamine and memantine [19, 62]. However, these drugs exhibited dose-dependent side effects and limited efficacy [50]. Therefore, currently there has been a growing focus on the use of traditional herbal medicines as an alternative therapy for AD.

In recent years, numerous studies have been published on acetylcholinesterase inhibitors. Many plants are renowned for their historical uses in various traditional practices as medicine with promising AChE inhibitory activity. That is why plant-based AChE inhibition has been kept at the center of attention for treating AD. Plants from the genus *Erythrina* is among the medical plants that have been long used for traditional medicine. Numerous studies have shown that extract from plants of genus *Erythrina* exhibited inhibitory activity against AChE, these including *Erythrina corallodendron* [47], *Erythrina caffra* [33], *Erythrina velutina* [49] and *Erythrina variegata* [41]. Moreover, the plants of genus *Erythrina* are also potential sources of antioxidant compounds, therefore they could be potential candidate to treat AD from natural products.

Erythrina crista-galli is one of the seasonal flowering plant species of genus *Erythrina* that are rich in secondary metabolites, particularly alkaloids and flavonoids [16, 17]. A number of secondary metabolites identified in this plant species have been reported to exhibit inhibitory effect on AChE, these are including vitexin [3], daidzein [60], genistein [15], erythraline, erythrinine, and cristanine A [33]. This highlights the potential role of *E. crista-galli* as natural source of AChE inhibitor. Nevertheless, reports on the secondary metabolite profile, especially in the flower of *E. crista-galli* are still limited, therefore, the exploration of metabolite profile and evaluation of their potency as AChE inhibitor for development of AD therapy from natural product is an intriguing and worthwhile topic to study.

2 Material and methods

2.1 Plant materials

The flowers of *E. crista-galli* were collected from Sersan Badjuri St., Bandung, West Jawa, Indonesia in December 2024. The plant materials have been determined at the Laboratory of Agricultural Production Technology & Services, Agricultural Cultivation Department, Faculty of Agriculture, University Padjadjaran under the voucher specimen number 1020 and was identified by Joko Kusmoro.

2.2 Extract preparation

The *E. crista-galli* flower (263 g) was dried in open air. The dried flowers were grinded into fine powder. The sample was then macerated with 96% methanol for 3 days and then filtered. The filter was then concentrated using rotary evaporator and stored before using.

2.3 DPPH free radical scavenging assay

The free radical scavenging activity of the methanol extract of *E. crista-galli* flower was evaluated using a 2,2-diphenyl-1-picrylhydrazyl (DPPH) radical scavenging assay, conducted on a 96-well microtiter plate, as outlined in previous research [5]. Different concentration (31.25 µg/mL–250 µg/mL) of the methanol extract of *E. crista-galli* flower was prepared using methanol as solvent. A mixture of 1.0 mM DPPH solution and 10 µL of the sample solution was added to each well of the microplate. The mixture was then left to react for 30 min in a dark room at room temperature. Following the reaction period, the absorbance of the solution was determined at a wavelength of 517 nm using a microplate reader. Methanol was used as the blank solution, while quercetin was used as a positive control. The percentage of DPPH activity inhibition was calculated using the following equation

$$\%\ \text{Inhibition} = \frac{(Absorbance\ of\ blank\ solution) - (Absorbance\ of\ test\ sample)}{Absorbance\ of\ blank\ solution} \text{x}\ 100\%$$

The IC_{50} value was obtained by plotting the sample concentration in the x axis against % inhibition in the y axis.

2.4 ABTS free radical scavenging assay

The ABTS free radical scavenging assay was conducted according to previous study [4]. The ABTS reagent was prepared by mixing 7 mM of ABTS stock solution with 2.45 mM

potassium persulfate in a proportion of 1:1. The reagent was let sit for 12–16 in the dark place before use. For the assay, the prepared ABTS solution was diluted with water to give absorbance of 0.7 at 734 nm. Different concentration (50 µg/mL–400 µg/mL) of the methanol extract of *E. crista-galli* flower was prepared using methanol as solvent. 1 mL of the sample solution was mixed with 3 mL of the ABTS solution. After 6 min reaction, the absorbance was measured at 734 nm. Methanol was used as the blank solution, while quercetin was used as a positive control. The percentage of ABTS activity inhibition was calculated using the following equation

$$\%\ \text{Inhibition}\ = \frac{(Absorbance\ of\ blank\ solution) - (Absorbance\ of\ test\ sample)}{Absorbance\ of\ blank\ solution} \text{x}\ 100\%$$

The IC_{50} value was obtained by plotting the sample concentration in the x axis against % inhibition in the y axis.

2.5 Ferric reducing/antioxidant power (FRAP)

The FRAP assay was conducted according to previous study [42]. The FRAP reagent was prepared by mixing 25 mL of sodium acetate trihydrate (0.3 M,pH 3.6) with 2.5 mL of 10 mM TPTZ solution (prepared in 40 mM HCl) and 2.5 mL of 20 mM of iron chloride aqueous solution to give a total of 30 mL FRAP solution. For the assay, 30 µL of the sample solution was reacted with 270 µL of FRAP reagent. After 5 min of reaction, the absorbance was measured in 595 nm. The results were expressed in mg quercetin/g extract, which was calculated by preparing a quercetin curve for FRAP assay (the standard curve equation: $y = 0.0416x + 0.1001$, $R^2 = 0.9983$) from 1.25 to 40 µg/mL of standard quercetin.

2.6 In vitro AChE inhibition activity

The in vitro AChE inhibitory activity of *E. crista-galli* methanol extract was evaluated using Ellman's method, as described in the literature [26]. Test solutions were prepared in buffer containing less than 10% methanol. The reaction mixture consisted of 125 µL DTNB (3 mM), 25 µL acetylcholine iodide (1.5 mM), 50 µL Tris–HCl buffer (50 mM, pH 8.0), and 25 µL sample, followed by the addition of 25 µL AChE solution (0.28 U/mL) in microwell plates. Absorbance was recorded at 405 nm at 5-s intervals for 2 min. Enzyme activity was calculated by comparing the reaction rate of the sample with that of the blank control, and inhibition (%) was determined as the difference between 100% and the measured enzyme activity.

2.7 Statistical analysis

Each in vitro experiment was carried out in triplicate, and the data are presented as mean values with their corresponding standard deviation (mean ± SD). Statistical analysis was limited to descriptive statistics, and no inferential tests were applied.

2.8 LC-MS/MS analysis

The separation of chemical constituents present in the extract of *E. crista-galli* flower was conducted using Ultra Performance Liquid Chromatography (UPLC) system (LC: ACQUITY UPLC® H-Class System, Waters, USA). A C18 column (1.8 µm 2.1 × 100 mm, ACQUITY UPLC® HSS, Waters, USA) was utilized for the analysis, maintained at a

column temperature of 50 °C and an ambient temperature of 25 °C. The mobile phase consisted of water with 5 mM ammonium formate (phase A) and acetonitrile with 0.05% formic acid (phase B). The flow rate was set to 0.2 mL/min using a step gradient method over a total run time of 23 min. An injection volume of 5 µL was employed, with samples filtered through a 0.2 µm syringe filter prior to injection.

Mass spectrometric analysis was performed using an electrospray ionization (ESI) system (Xevo G2-S QTof, Waters, USA). The mass analysis range was set from 50 to 1200 m/z. The source temperature was maintained at 100 °C, while the desolvation temperature was set to 350 °C with a desolvation gas flow rate of 793 L/hr. The collision energy was set at 4 V for low-energy analysis, with a ramp collision energy between 25 to 60 V. Leucine enkephalin was used for internal mass correction and was infused every 10 s throughout the run.

Data processing was caried out using MassLynx software (version 4.1). Compound annotation was performed by comparing the molecular formula suggested by the MassLynx software from the HR-MS data (mass error < 10 ppm) with the molecular formula data of 729 secondary metabolites previously isolated from genus *Erythrina*.

2.9 Molecular docking

The 3D structure of Human Acetylcholinesterase in complex with (-)-galantamine was downloaded from the Protein Data Bank (PDB) under the ID 4EY6 (https://www.rcsb.org/structure/4ey6). The co-crystallized ligand was separated from the protein complex using Biovia Discovery Studio (DS) 2021 Client software, and both structures (the co-crystallized and ligand-free protein) were saved as pdb file format. Subsequently, these files were prepared for redocking using AutoDockTools 1.5.6 and saved as pdbqt file format. Following, the co-crystallized ligand and ligand-free protein were redocked using AutoDock4 (v4.2.6).

The two-dimensional (2D) structures of the chemical components identified in the methanol extract of *E. crista-galli* flowers from LC-MS/MS analysis were sketched using Chemaxon MarvinSketch software. The protonation state of each structure at physiological pH (7.4) was also predicted with Chemaxon MarvinSketch. Subsequently, the three-dimensional (3D) structures of each compound were generated and optimized using the MMFF94 force field in Avogadro software, and then saved as pdb files. These 3D structures were prepared for molecular docking using AutoDockTools 1.5.6 and saved in pdbqt format. The molecular docking was then performed following the same procedure as the redocking process.

2.10 Molecular dynamics simulation

Molecular dynamics simulation was conducted according to our previous research [1, 24]. Prior to the simulation, the histidine residues in the protein structure were adjusted using the pdb4amber program, taking into account their local chemical environments, and assigned to the ff19SB force field. The partial charges of the ligand structures were assigned using the Austin Model 1-Bond Charge (AM1-BC) method from the antechamber tool in AmberTools21, followed by ligand parameterization with the Generalized Amber Force Fields 2 (GAFF2). The ligand–protein complex was then prepared using the tleap program from AmberTools21. To solvate the complex, the TIP3P explicit

water model with a minimal boundary box of 10 Å was used, followed by the addition of Na^+ and Cl^- ions to achieve a physiological salt concentration of 0.15 M.

The Particle-Mesh Ewald Molecular Dynamics (PMEMD) module in AMBER20 with GPU acceleration was utilized to run the molecular dynamics simulation. The minimization of the ligand–protein complex was conducted with two sequential steps. The initial minimization process consisted of 1000 steps using the steepest descent method and 2000 steps using the conjugate gradient method, with a harmonic force of 5 kcal mol^{-1} $Å^{-2}$ applied. This was followed by 5000 steps of unrestricted conjugate gradient minimization to correct any spatial overlaps. The system's temperature was gradually increased to 300 K in increments of 20 ps (0–100 K; 100–200 K; and 200–300 K) over a total duration of 60 ps. An equilibration period was performed to ensure consistent density and pressure, with a gradual release of force over 1000 ps. The production runs were then conducted for 100 ns, with each step lasting 2 fs [23].

3 Result

3.1 Free radical scavenging and acetylcholinesterase inhibition activities of *E. crista-galli* flowers extract

Methanol extract from *E. crista-galli* flowers was evaluated using DPPH, ABTS, and FRAP methods. The methanol extract exhibited IC_{50} of 153.6 ± 2.4 µg/ml in DPPH assay, while 255.7 ± 14.9 µg/ml in ABTS assay, and 25.4 ± 1.8 mgQE/g extract in FRAP assay. The standard quercetin exhibited significant free radical scavenging activity with IC_{50} of 8.21 ± 0.06 µg/ml in DPPH assay, and 4.04 ± 0.73 µg/ml in ABTS assay. The methanol extract inhibited 17.65 ± 1.28% of the AChE activity at the concentration of 50 µg/ml, whereas galantamine as positive control exhibited IC_{50} of 0.36 ± 0.2 µg/mL.

3.2 Metabolite profile of *E. crista-galli* methanol extract

The interpretation of LCMS/MS both in positive and negative ion modes (Fig. 1) data followed by careful examination and comparison with literature data has led to tentative identification of erythrina-type alkaloids along with flavonoids in the methanol extract of *E. crista-galli* flower (Table 1). The identification was based on the calculated molecular formula derived from the mass spectra, with mass error of less than 5 ppm. These molecular formulas were then matched with those of Erythrina alkaloids and flavonoids reported in the literatures. Furthermore, this tentative identification was supported by the presence of characteristic fragmentations in the MS/MS spectra, particularly the $[M+H–CH_3OH]^+$ and $[M+H–C_3H_6O]^+$ fragments, which are typical of both dienoid and alkenoid types of Erythrina alkaloids [7, 21].

In addition to erythrina type alkaloids, a number of C-glycosylated flavonoids were also tentatively identified in the methanol extract of *E. crista-galli* flower from negative ion mode. These compounds give characteristics fragment ions at $[M-H-90]^-$ and $[M-H-120]^-$ which correspond to $^{0,3}X$ dan $^{0,2}X$ cross-ring cleavage of the sugar moiety [28, 36].

3.3 Molecular docking

Molecular docking was employed to screen the potency of secondary metabolites identified by LC-MS/MS analysis in the methanol extract of *E crista-galli* flower to inhibit acetylcholinesterase. Molecular docking for virtual screening was conducted using autodock4 as this docking program have been reported to provide more accurate

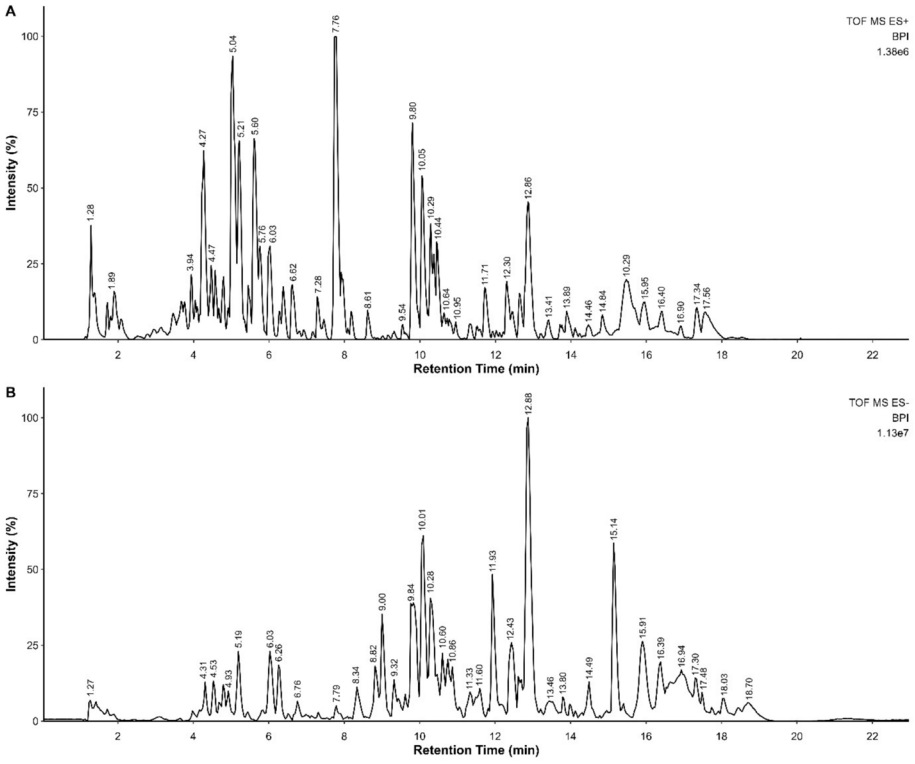


Fig. 1 Chromatogram in positive ion mode **A** and negative ion mode **B** analysis

binding affinity prediction [34]. Prior to the docking procedure, we performed a redocking procedure of the co-crystallized ligand to validate the accuracy and reliability of the docking protocol by checking if the docking protocol can reproduce the experimentally observed binding mode. The redocking procedure yielded an RMSD of 0.68 Å, which implies that the molecular docking protocol is valid. The binding affinity of the secondary metabolites identified in the flower of *E. crista-galli* against AChE is given in Table S1 (supplementary material). Among these secondary metabolites, vicenin-2 and vitexin are the top two with the lowest docking score (– 13.02 and – 11.80 kcal/mol respectively), even lower than that of galantamine (– 9.39 kcal/mol). These results suggest that both vicenin-2 and vitexin may poses strong potential as AChE inhibitor. The binding pose of vicenin-2 and vitexin (Fig. 2) demonstrate the interaction of these compounds with amino acids in the catalytic and peripheral residues of AChE. These are including hydrogen bond with Tyr337 and Tyr124 which are parts of the PAS residue.

3.4 Molecular dynamics simulation

The results of the 100 ns molecular dynamics simulation provide insights into the stabilizing effects of vicenin-2 and vitexin on acetylcholinesterase (AChE). Specifically, the AChE – Vitexin complex exhibited median RMSD of 1.571 ± 0.133 Å, while the AChE – Vicenin2 complex exhibited a slightly higher median RMSD of 1.682 ± 0.163 Å. These RMSD values are notably lower than the RMSD of the Apo form of AChE, which was measured at 1.783 ± 0.321 Å. Moreover, the binding energy of AChE – Vicenin2 complex obtained from MMGBSA calculation was – 32.104 ± 7.73 kcal·mol^{-1}, whereas AChE – Vitexin was – 31.166 ± 1.83 kcal·mol^{-1}. Though, their binding energies are higher than that of galantamine (– 42.85 ± 3.22 kcal·mol^{-1}), which a known

Table 1 Alkaloids and flavonoids identified in *E. crista-galli* flowers

RT	m/z	Molecular formula	Mass error (ppm)	Fragments	Compound	Source
Positive ion mode						
3.94	332.1500	$C_{18}H_{21}NO_5$	0.6	314; 300; 282; 254; 226	Cristanine D (1)	*E. crista-galli* [39]
4.47	312.1245	$C_{18}H_{17}NO_4$	2.9	280; 262; 232; 204	8-oxoerythraline (2)	E. crista-galli [55]
4.57	316.1559	$C_{18}H_{21}NO_4$	3.2	-	Erythratine (3)	*E. crista-galli* [55]
4.66	332.1861	$C_{19}H_{25}NO_4$	0.3	314; 264; 178	Erythratidine (4)	*E. crista-galli* [55]
4.80	330.1709	$C_{19}H_{23}NO_4$	1.2	-	Erysotrine N-Oxide (5)	*E. crista-galli* [55]
4.86	344.1504	$C_{19}H_{21}NO_5$	1.7	-	Cristanine C (6)	*E. crista-galli* [55]
4.95	328.1554	$C_{19}H_{21}NO_4$	1.5	-	Erysotramidine (7)	*E. crista-galli* [55]
5.04	314.1400	$C_{18}H_{19}NO_4$	2.5	264; 234	Erythrinine (8)	*E. crista-galli* [55]
5.21	372.1454	$C_{20}H_{21}NO_6$	1.9	322; 262	11-methoxy-10-oxoerysotramidine (9)	*E. latissimi* [11]
5.45	344.186	$C_{20}H_{25}NO_4$	0.6	344	Erythristemine (10)	*E. stricta* [58]
5.6	298.1451	$C_{18}H_{19}NO_3$	2.7	266; 236; 208	Erythraline (11)	*E. crista-galli* [55]
5.76	356.1502	$C_{20}H_{21}NO_5$	1.1	264; 324	Eryalkal C (12)	*E. crista-galli* [59]
6.03	386.1611	$C_{21}H_{23}NO_6$	1.8	336; 262; 276	8-acetatemethoxyerythranine (13)	*E. crista-galli* [59]
6.62	310.1092	$C_{18}H_{15}NO_4$	4.2	278; 250	Cristamidine (14)	*E. crista-galli* [55]
7.45	328.119	$C_{18}H_{17}NO_5$	1.5	278; 250; 220	8-Oxoerythrinine (15)	*E. crista-galli* [55]
7.76	326.1034	$C_{18}H_{15}NO_5$	1.8	294; 266; 236	10,11-Dioxoerythraline (16)	*E. collarodendron* [61]
Negative ion mode						
4.31	593.1504	$C_{27}H_{30}O_{15}$	0.3	473, 383, 353	vicenin-2 (17)	*E. falcata* [13]
4.53	563.1388	$C_{26}H_{28}O_{14}$	2.3	473; 443; 383; 353; 297	apigenin 6-C-glucosyl-8-C-arabinoside (18)	[9]
4.93	431.0972	$C_{21}H_{20}O_{10}$	1.4	357; 311; 283; 269	Vitexin (19)	*E. falcata* [13]
6.76	253.0497	$C_{15}H_{10}O_4$	1.6	225; 209 135	Daidzein (20)	*E. crista-galli* [45]
7,79	269,0457	$C_{15}H_{10}O_5$	2,6	151; 241; 225; 197	Genistein (21)	*E. crista-galli* [45]

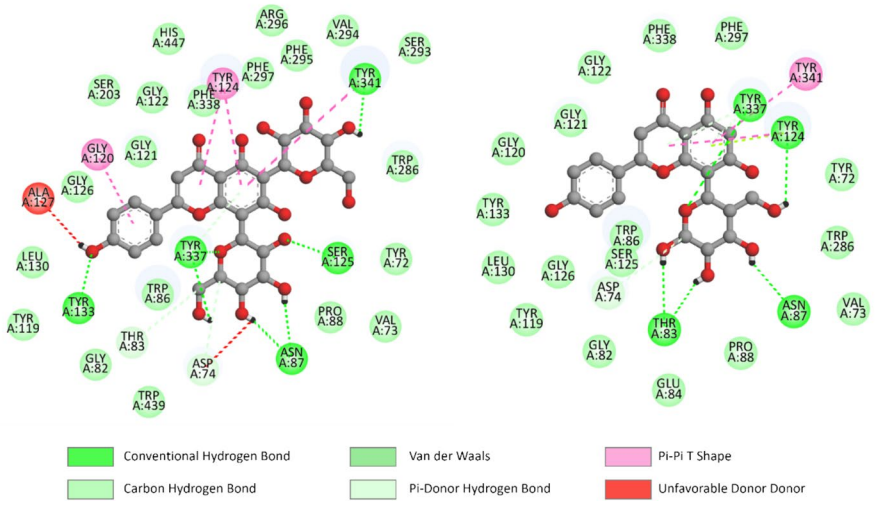


Fig. 2 Interaction of vicenin-2 (left) and vitexin (right) with amino acids of the AChE

inhibitor of AChE, these complexes exhibited lower binding energy than the acetylcholine (-24.33 ± 3.57 kcal·mol^{-1}), which is the natural substrate of AChE.

4 Discussion

This study aims to evaluate the potency of *E. crista-galli* flower as a remedy for AD therapy through free radical scavenging activity and inhibition of acetylcholinesterase. Free radical scavengers, play a crucial role in mitigating oxidative stress [29], which is a significant factor in the pathogenesis of AD [8]. The moderate free radical scavenging activity of *E. crista-galli* flower suggest that secondary metabolites present in the extract are capable of neutralizing free radicals thus preventing cellular damage and protect neuronal cells from oxidative stress-induced apoptosis.

LC-MS/MS analysis of the methanol extract of *E. crista-galli* flower revealed the presence of erythrina alkaloids along with flavonoids (Fig. 3). Among these secondary metabolites, vitexin and have been reported to exhibit free radical scavenging activity [22, 27, 30]. Moreover, these compounds also inhibit various oxidative stress markers and enzymes, such as superoxide dismutase and catalase, contributing to its protective effects against oxidative damage [40, 54], further support that the methanol extract of *E. crista-galli* flower could potentially reduce oxidative stress in AD patients.

In addition to oxidative stress, cholinergic dysfunction is another key factor in AD pathophysiology [43]. To evaluate the cholinergic inhibitory potency of *E. crista-galli*

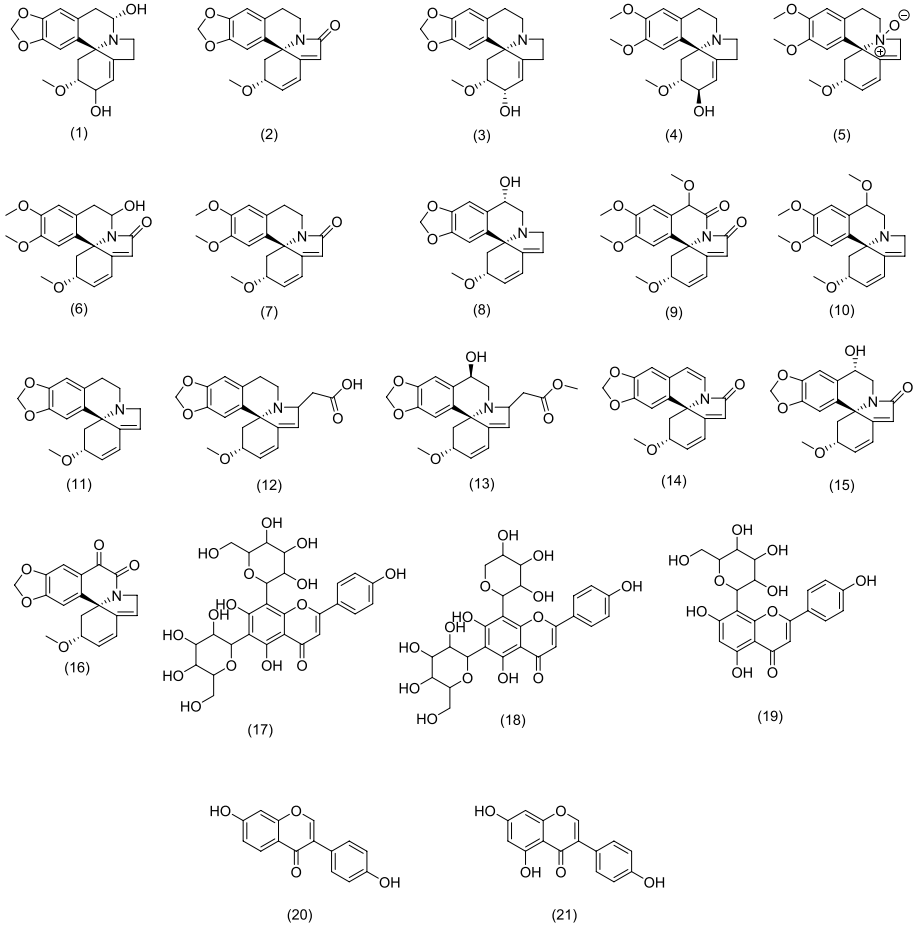


Fig. 3 Secondary metabolites tentatively identified in *E. crista-galli* flowers

flower extract, the secondary metabolites identified in *E. crista-galli* flower were subjected to molecular docking against AChE. The virtual screening revealed that the majority of compounds identified in the flowers of *E. crista-galli* exhibit potential as AChE inhibitors, attributable to their lower binding affinities relative to acetylcholine. Notably, some compounds even demonstrate lower binding affinities than galantamine, a known AChE inhibitor. Of these secondary metabolites, vitexin and genistein have been documented to inhibit AChE activity in vitro [31, 52, 60]. To further elucidate the inhibitory potential of these compounds, we performed molecular dynamics simulations on the top candidates (vicenin-2 and vitexin) to assess their binding interactions and effects on AChE stability.

The results of the 100 ns molecular dynamics simulation provide insights into the stabilizing effects of vicenin-2 and vitexin on acetylcholinesterase (AChE). Both AChE – Vicenin2 and vitexin complexes exhibited lower RMSD values compared to the apo form of AChE (Fig. 4). The lower RMSD values for the compound-bound forms of AChE suggest that the presence of these ligands results in reduced structural fluctuations of the enzyme [20]. This implies that both vicenin-2 and vitexin confer a stabilizing effect on AChE, helping to maintain its structural integrity during the simulation period. The stabilizing effects of vicenin-2 and vitexin also highlight their potential utility in therapeutic applications, where enzyme stability is crucial for effective inhibition and activity modulation (Fig. 5).

Apart from ligand–protein binding stability, molecular dynamics simulation can also provide valuable information on the thermodynamics and kinetics of binding, including the calculation of binding free energies and the identification of key interactions that stabilize the complex [51]. The binding energy of AChE – Vicenin2 and AChE – Vitexin complexes obtained from MMGBSA calculation exhibited lower binding energy than the AChE – Galantamine complex. Lower MMGBSA free energy values indicate a more favorable binding interaction between the compound and the protein, suggesting higher binding stability [56]. This increased stability is crucial for effective inhibition, as it means the inhibitor remains bound to the target protein for a longer duration, thereby exerting its inhibitory effect more efficiently [53]. Consequently, vicenin-2 and vitexin,

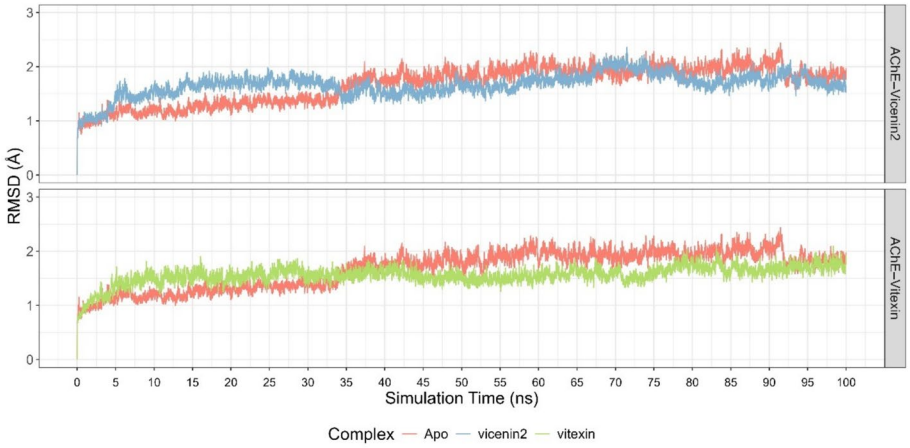


Fig. 4 RMSD Plot Comparison of AChE in Apo Form (pink), AChE–Vitexin Complex (lime green), and AChE–Vicenin-2 Complex (blue)

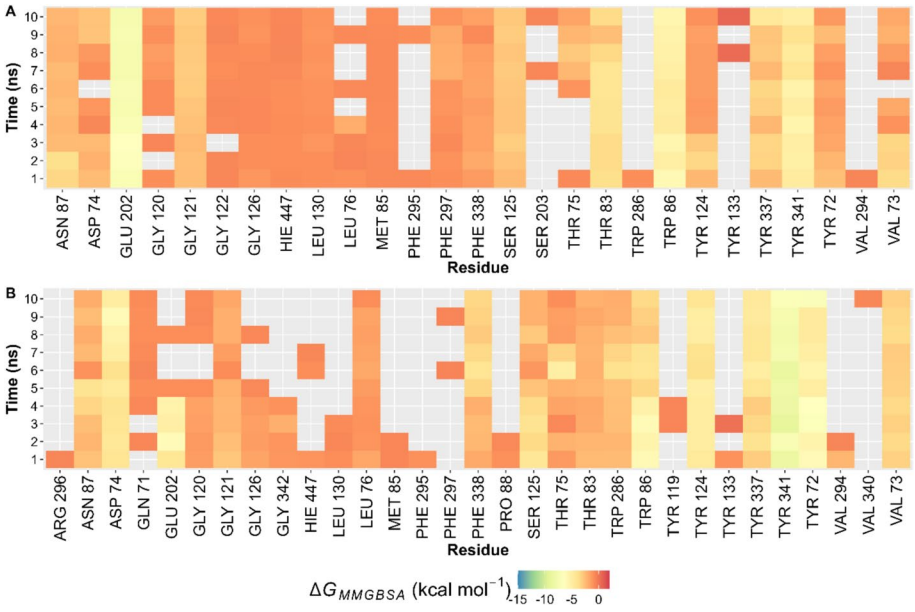


Fig. 5 Heatmaps of MMGBSA binding energy decomposition for residues of AChE interacting with vitexin (**A**) and vicenin-2 (**B**)

with their lower binding energies, are likely to have greater inhibitory potency against AChE compared to Galantamine.

In addition to MMGBSA free energy calculation, residue-based energy decomposition was also performed in order to identify the amino acid residue within the AChE binding pocket which contribute to stabilize the AChE – Vitexin and AChE – Vicenin2 complexes. In residue-based energy decomposition, the residue within the binding pocket is regarded as an important residue in the molecular recognition of a ligand if the interaction energy between a residue and the ligand is lower than – 0.8 kcal/mol [18]. This analysis allows for pinpointing key residues that play significant roles in ligand binding and stabilization, providing deeper insights into the molecular interactions governing the efficacy of these compounds as potential AChE inhibitors.

For the AChE – vitexin complex, several key residues play significant roles in molecular recognition, particularly within the anionic subsite that binds the quaternary trimethylammonium choline moiety of acetylcholine. Notably, Glu^{202} (– 7.36 kcal/mol) and Trp^{86} (– 5.11 kcal/mol), and Tyr^{337} (– 2.97 kcal/mol) exhibit low binding affinities when interacting with vitexin. Similarly, in the AChE – Vicenin2 complex, strong interaction with Tyr^{337} (– 4.20 kcal/mol), Trp^{86} (– 4.09 kcal/mol), and Glu^{202} (– 0,86 kcal/mol). These interactions, particularly at the anionic subsite, indicates that both compounds could bind effectively to the active site of AChE, thereby inhibiting acetylcholine hydrolysis. This mechanism suggests their potential as AChE inhibitor, which may contribute to symptomatic relief in neurogenerative condition such as AD.

Based on the result of antioxidant activity, anti-cholinesterase inhibitory evaluation, metabolite profiling, and virtual screening through molecular docking and molecular dynamics simulation, the methanol extract of *E. crista-galli* flower demonstrates promising potential as a source of bioactive compounds with acetylcholinesterase inhibitory activity. Query Regarding the safety of the extract for human consumption, though there is limited literature reporting toxicity of extract derived from *E. crista-galli*, number of

research have demonstrated that extract derived from another species of genus *Erythrina* such as *E. senegalensis, E. variegata, E. veluntina, E. sacleuxii,* and *E. fusca* are safe for human consumptions [12, 25, 32, 35, 37].

5 Conclusion

This study presents the metabolite profile, antioxidant capacity, and acetylcholinesterase (AChE) inhibitory activity of *E. crista-galli* flower extract through both in vitro and in silico studies. The methanol extract exhibited moderate antioxidant activity, with IC50 values of 153.6 ± 2.4 µg/ml (DPPH) and 255.7 ± 14.9 µg/ml (ABTS), and a FRAP value of 25.4 ± 1.8 mgQE/g extract. It also demonstrated AChE inhibition of 17.65 ± 1.28% at a concentration of 50 µg/ml. Metabolite profiling via LC-MS/MS identified 16 erythrina alkaloids and 5 flavonoids in the extract. Furthermore, molecular docking and molecular dynamics simulations highlighted vicenin-2 and vitexin as key compounds with strong binding affinity toward AChE, supporting their potential as natural AChE inhibitors.

Abbreviations

AChE	Acetylcholinesterase
AD	Alzheimer's disease
LCMS	Liquid chromatography-mass spectrometry
MMGBSA	Molecular mechanics, general born surface area
RMSD	Root mean square deviation

Supplementary Information

The online version contains supplementary material available at https://doi.org/10.1007/s42452-025-07964-5.

Supplementary file 1.

Acknowledgements
We would like to thank Universitas Padjadjaran for all the supports and funding

Author contributions
Abd. Wahid Rizaldi Akili: Investigation, formal analysis, software, writing original draft; Gian Primahana: Formal analysis, data curation, investigation; Sofa Fajriah: Data curation, formal analysis, investigation; Ari Hardianto: Data curation, writing, review, and editing; Jalifah Latip: Validation, writing, review, and editing; Tati Herlina: Funding acquisition, visualization, resources, validation, writing, review, and editing.

Funding
Open access funding provided by University of Padjadjaran. This research was funded by Universitas Padjadjaran through the Beasiswa Unggulan Pascasarjana Padjadjaran (BUPP) scheme (No.1936/UNG.3.1/PT.00/2024) by Tati Herlina.

Data availability
The datasets used and/or analysed during the current study are available from the corresponding author on reasonable request.

Declarations

Ethics approval and consent to participate
Not applicable.

Consent for publication
Not applicable.

Competing interests
The authors declare no competing interests.

Received: 27 February 2025 / Accepted: 5 November 2025
Published online: 29 December 2025

References

1. Akili AWR, Thurfah NA, Hardianto A, et al. Investigating the potency of Erythrina-derived flavonoids as cholinesterase inhibitors and free radical scavengers through in silico approach: implications for Alzheimer's disease therapy. Adv Appl Bioinform Chem. 2024;17:107–18. https://doi.org/10.2147/AABC.S483115.
2. Alzheimer's disease facts and figures (2024) https://www.alz.org/alzheimers-dementia/facts-figures
3. Babaei F, Moafizad A, Darvishvand Z, et al. Review of the effects of vitexin in oxidative stress-related diseases. Food Sci Nutr. 2020;8:2569–80. https://doi.org/10.1002/fsn3.1567.
4. Bari MdW, Islam A, Islam MdM, et al. Determination of in vitro antioxidant activity and in vivo antineoplastic effects against Ehrlich ascites carcinoma of methanolic extract of *Sphagneticola calendulacea* (L.) Pruski. Heliyon. 2021;7:e07228. https://doi.org/10.1016/j.heliyon.2021.e07228.
5. Bedane KG, Kusari S, Eckelmann D, et al. Erylivingstone A-C with antioxidant and antibacterial activities from *Erythrina livingstoniana*. Fitoterapia. 2015. https://doi.org/10.1016/j.fitote.2015.06.016.
6. Bekdash RA. The cholinergic system, the adrenergic system and the neuropathology of Alzheimer's disease. Int J Mol Sci. 2021. https://doi.org/10.3390/ijms22031273.
7. Boar RB, Widdowson DA (1970) Mass spectra of the Erythrina alkaloids: a novel fragmentation of the spiran system. J Chem Soc B 1591–1595. https://doi.org/10.1039/J29700001591
8. Buccellato FR, D'Anca M, Galimberti D, et al. Role of oxidative damage in Alzheimer's disease and neurodegeneration: from pathogenic mechanisms to biomarker discovery. Antioxidants. 2021. https://doi.org/10.3390/antiox10091353.
9. Cao J, Yin C, Qin Y, et al. Approach to the study of flavone di-C-glycosides by high performance liquid chromatography-tandem ion trap mass spectrometry and its application to characterization of flavonoid composition in *Viola yedoensis*. J Mass Spectrom. 2014;49:1010–24. https://doi.org/10.1002/jms.3413.
10. Chen ZR, Huang JB, Yang SL, Hong FF. Role of cholinergic signaling in Alzheimer's disease. Molecules. 2022. https://doi.org/10.3390/molecules27061816.
11. Cornelius WW, Akeng'a T, Obiero GO, Lutta KP (2009) Antifeedant activities of the erythrinaline alkaloids from Erythrina latissima against Spodoptera littoralis (Lepidoptera noctuidae). Records of Natural Products 3:
12. de Bona AP, Batitucci MCP, Andrade MA, et al. Estudo fitoquímico e análise mutagênica das folhas e inflorescências de Erythrina mulungu (Mart. ex Benth.) através do Teste de Micronúcleo em roedores. Rev Bras Plantas Med. 2012. https://doi.org/10.1590/S1516-05722012000200014.
13. de Oliveira DR, Zamberlam CR, Gaiardo RB, et al. Flavones from *Erythrina falcata* are modulators of fear memory. BMC Complement Altern Med. 2014. https://doi.org/10.1186/1472-6882-14-288.
14. Dhapola R, Beura SK, Sharma P, et al. Oxidative stress in Alzheimer's disease: current knowledge of signaling pathways and therapeutics. Mol Biol Rep. 2024. https://doi.org/10.1007/s11033-023-09021-z.
15. Duan X, Li Y, Xu F, Ding H. Study on the neuroprotective effects of Genistein on Alzheimer's disease. Brain Behav. 2021. https://doi.org/10.1002/brb3.2100.
16. Fahmy NM, Al-Sayed E, El-Shazly M, Nasser Singab A. Alkaloids of genus *Erythrina*: an updated review. Nat Prod Res. 2020;34:1891–912. https://doi.org/10.1080/14786419.2018.1564300.
17. Fahmy NM, Al-Sayed E, El-Shazly M, Singab AN. Comprehensive review on flavonoids biological activities of *Erythrina* plant species. Ind Crops Prod. 2018;123:500–38. https://doi.org/10.1016/j.indcrop.2018.06.028.
18. Fang J, Wu P, Yang R, et al. Inhibition of acetylcholinesterase by two genistein derivatives: kinetic analysis, molecular docking and molecular dynamics simulation. Acta Pharm Sin B. 2014. https://doi.org/10.1016/j.apsb.2014.10.002.
19. Fedeli C, Filadi R, Rossi A, et al. PSEN2 (presenilin 2) mutants linked to familial Alzheimer disease impair autophagy by altering Ca2+ homeostasis. Autophagy. 2019. https://doi.org/10.1080/15548627.2019.1596489.
20. Ghahremanian S, Rashidi MM, Raeisi K, Toghraie D. Molecular dynamics simulation approach for discovering potential inhibitors against SARS-CoV-2: a structural review. J Mol Liq. 2022. https://doi.org/10.1016/j.molliq.2022.118901.
21. Guaratini T, Feitosa LGP, Silva DB, et al. Gas-phase dissociation study of erythrinian alkaloids by electrospray ionization mass spectrometry and computational methods. J Mass Spectrom. 2017;52:571–9. https://doi.org/10.1002/jms.3962.
22. Guo Q, Rimbach G, Moini H, et al. ESR and cell culture studies on free radical-scavenging and antioxidant activities of isoflavonoids. Toxicology. 2002. https://doi.org/10.1016/S0300-483X(02)00241-X.
23. Hardianto A, Mardetia SS, Destiarani W, et al. Unveiling the anti-cancer potential of onoceranoid triterpenes from *Lansium domesticum* Corr. cv. kokosan: an in silico study against estrogen receptor alpha. Int J Mol Sci. 2023. https://doi.org/10.3390/ijms241915033.
24. Herlina T, Akili AWR, Nishinarizki V, et al. Cytotoxic evaluation, molecular docking, molecular dynamics, and ADMET prediction of isolupalbigenin isolated from *Erythrina subumbrans* (Hassk). Merr. (Fabaceae) stem bark: unveiling its anticancer efficacy. Onco Targets Ther. 2024;17:829–40. https://doi.org/10.2147/OTT.S482469.
25. Herlina T, Madihah M, Deni D, Amien S. Subchronic toxicity of methanol extract from *Erythrina variegata* (Leguminosae) leaves on male Wistar rats (*Rattus norvegicus*). Molekul. 2017. https://doi.org/10.20884/1.jm.2017.12.1.349.
26. Ingkaninan K, Changwijit K, Suwanborirux K. Vobasinyl-iboga bisindole alkaloids, potent acetylcholinesterase inhibitors from *Tabernaemontana divaricata* root. J Pharm Pharmacol. 2006;58:847–52. https://doi.org/10.1211/jpp.58.6.0015.
27. Javed Z, Khan K, Herrera-Bravo J, et al. Genistein as a regulator of signaling pathways and microRNAs in different types of cancers. Cancer Cell Int. 2021. https://doi.org/10.1186/s12935-021-02091-8.
28. Kachlicki P, Piasecka A, Stobiecki M, Marczak Ł. Structural characterization of flavonoid glycoconjugates and their derivatives with mass spectrometric techniques. Molecules. 2016. https://doi.org/10.3390/molecules21111494.
29. Kurutas EB. The importance of antioxidants which play the role in cellular response against oxidative/nitrosative stress: current state. Nutr J. 2016. https://doi.org/10.1186/s12937-016-0186-5.
30. Li H, Cao D, Yi J, et al. Identification of the flavonoids in mungbean (*Phaseolus radiatus* L.) soup and their antioxidant activities. Food Chem. 2012. https://doi.org/10.1016/j.foodchem.2012.07.048.
31. Malar DS, Shafreen RB, Pandian SK, Devi KP. Cholinesterase inhibitory, anti-amyloidogenic and neuroprotective effect of the medicinal plant *Grewia tiliaefolia* - an in vitro and in silico study. Pharm Biol. 2017. https://doi.org/10.1080/13880209.2016.1241811.
32. Mwanasiti OM, Florence AN, Mutinda CK, Esther NM. Phytochemical analysis and safety evaluation of ethanol roots extract of *Erythrina sacleuxii* Hua in Wistar albino rats. J Med Plants Res. 2022. https://doi.org/10.5897/jmpr2021.7204.

33. Nassief SM, Amer ME, Shawky E, et al. Acetylcholinesterase inhibitory alkaloids from the flowers and seeds of *Erythrina caffra*. Rev Bras Farmacogn. 2020;30:859–64. https://doi.org/10.1007/s43450-020-00114-5.
34. Nguyen NT, Nguyen TH, Pham TNH, et al. Autodock Vina adopts more accurate binding poses but Autodock4 forms better binding affinity. J Chem Inf Model. 2020;60:204–11. https://doi.org/10.1021/acs.jcim.9b00778.
35. Nhung TTP, Quoc LPT (2023) Acute and sub-chronic toxicity studies of the ethanol extract of Erythrina fusca Lour. fruit via oral administration in mice. Acta Biologica Szegediensis 67. https://doi.org/10.14232/abs.2023.1.111-122
36. Ni R, Liu XY, Zhang JZ, et al. Identification of a flavonoid C-glycosyltransferase from fern species *Stenoloma chusanum* and the application in synthesizing flavonoid C-glycosides in *Escherichia coli*. Microb Cell Fact. 2022;21:210. https://doi.org/10.1186/s12934-022-01940-z.
37. Njayou F, Moundipa P, Donfack J, et al (2010) Hepato-protective, antioxidant activities and acute toxicity of a stem bark extract of Erythrina senegalensis DC. Int J Biol Chem Sci 4. https://doi.org/10.4314/ijbcs.v4i3.60503
38. Olufunmilayo EO, Gerke-Duncan MB, Holsinger RMD. Oxidative stress and antioxidants in neurodegenerative disorders. Antioxidants. 2023. https://doi.org/10.3390/antiox12020517.
39. Ozawa M, Kawamata S, Etoh T, et al. Structures of new erythrinan alkaloids and nitric oxide production inhibitors from *Erythrina crista-galli*. Chem Pharm Bull (Tokyo). 2010;58:1119–22. https://doi.org/10.1248/cpb.58.1119.
40. Park CE, Yun H, Lee EB, et al. The antioxidant effects of genistein are associated with AMP-activated protein kinase activation and PTEN induction in prostate cancer cells. J Med Food. 2010. https://doi.org/10.1089/jmf.2009.1359.
41. Patil VS, Meena H, Harish DR. *Erythrina variegata* L. bark: an untapped bioactive source harbouring therapeutic properties for the treatment of Alzheimer's disease. In Silico Pharmacol. 2021. https://doi.org/10.1007/s40203-021-00110-0.
42. Pereira ACH, Lenz D, Nogueira BV, et al. Gastroprotective activity of the resin from *Virola oleifera*. Pharm Biol. 2017;55:472–80. https://doi.org/10.1080/13880209.2016.1251467.
43. Petrova T, Orellana C, Jelic V, et al. Cholinergic dysfunction, neurodegeneration, and amyloid-beta pathology in neurodegenerative diseases. Psychiatry Res Neuroimaging. 2020. https://doi.org/10.1016/j.pscychresns.2020.111099.
44. Ramachandran AK, Das S, Joseph A, et al (2020) Neurodegenerative pathways in Alzheimer's Disease: a review. Curr Neuropharmacol 19:. https://doi.org/10.2174/1570159x18666200807130637
45. Redko F, Clavin ML, Weber D, et al. Antimicrobial isoflavonoids from *Erythrina crista galli* infected with *Phomopsis* sp. Z Naturforsch C. 2007;62:164–8. https://doi.org/10.1515/znc-2007-3-402.
46. Roy RG, Mandal PK, Maroon JC. Oxidative stress occurs prior to amyloid Aβ plaque formation and tau phosphorylation in Alzheimer's disease: role of glutathione and metal ions. ACS Chem Neurosci. 2023;14:2944–54. https://doi.org/10.1021/acschemneuro.3c00486.
47. Salem AM, Mostafa NM, Al-Sayed E, et al. Insights into the role of *Erythrina corallodendron* L. in Alzheimer's disease: in vitro and in silico approach. Chem Biodivers. 2023. https://doi.org/10.1002/cbdv.202300200.
48. Salim S. Oxidative stress and the central nervous system. J Pharmacol Exp Ther. 2017. https://doi.org/10.1124/jpet.116.237503.
49. Santos WP, Da Silva Carvalho AC, Dos Santos Estevam C, et al. In vitro and ex vivo anticholinesterase activities of *Erythrina velutina* leaf extracts. Pharm Biol. 2012;50:919–24. https://doi.org/10.3109/13880209.2011.649429.
50. Sharma K. Cholinesterase inhibitors as Alzheimer's therapeutics (Review). Mol Med Rep. 2019. https://doi.org/10.3892/mmr.2019.10374.
51. Shukla R, Tripathi T (2020) Molecular Dynamics Simulation of Protein and Protein-Ligand Complexes. In: Computer-Aided Drug Design.
52. Singh NK, Verma N, Gupta JK, Raghav J (2024) Anti-amnesic and Neuroprotective Potential of Genistein Against Alzheimer's Disease. Revista Brasileira de Farmacognosia 34.
53. Spassov DS. Binding affinity determination in drug design: insights from lock and key, induced fit, conformational selection, and inhibitor trapping models. Int J Mol Sci. 2024;25:7124. https://doi.org/10.3390/ijms25137124.
54. Ubaid M, Salauddin N, Shadani MA, et al (2023) Daidzein from Dietary Supplement to a Drug Candidate: An Evaluation of Potential. ACS Omega 8.
55. Wang D, Xie N, Yi S, et al. Bioassay-guided isolation of potent aphicidal *Erythrina* alkaloids against *Aphis gossypii* from the seed of *Erythrina crista-galli* L. Pest Manag Sci. 2017;74:210–8. https://doi.org/10.1002/ps.4698.
56. Wang E, Sun H, Wang J, et al. End-point binding free energy calculation with MM/PBSA and MM/GBSA: strategies and applications in drug design. Chem Rev. 2019. https://doi.org/10.1021/acs.chemrev.9b00055.
57. World Health Organization (2025) Dementia. In: https://www.who.int/news-room/fact-sheets/detail/dementia#:~:text=WHO%20recognizes%20dementia%20as%20a,individuals%20to%20facilitate%20action%20globally.
58. Wu J, Zhang B-J, Bao M-F, Cai X-H. A new erythrinan N-oxide alkaloid from *Erythrina stricta*. Nat Prod Res. 2019;33:2004–10. https://doi.org/10.1080/14786419.2018.1483924.
59. Zhang BJ, Wu J, Bao MF, et al. Artificial Erythrina alkaloids from three *Erythrina* plants, *E. variegata*, *E. crista-galli* and *E. arborescens*. Nat Prod Bioprospect. 2020. https://doi.org/10.1007/s13659-020-00235-3.
60. Zhang J, Kowsalya R. Daidzein ameliorates cerebral ischemic-reperfusion induced neuroinflammation in Wistar rats via inhibiting NF-κB signaling pathway. Pharmacogn Mag. 2023. https://doi.org/10.1177/09731296221137378.
61. Zhao HE, Wu J, Xu FQ, et al. Alkaloids from flowers of *Erythrina corallodendron*. Nat Prod Res. 2019. https://doi.org/10.1080/14786419.2018.1472596.
62. Zhu J, Wang LN, Cai R, et al. Design, synthesis, evaluation and molecular modeling study of 4-N-phenylaminoquinolines for Alzheimer disease treatment. Bioorg Med Chem Lett. 2019. https://doi.org/10.1016/j.bmcl.2019.03.050.

Publisher's Note

Springer Nature remains neutral with regard to jurisdictional claims in published maps and institutional affiliations.